Lotfy *et al. Egypt J Radiol Nucl Med (2024) 55:111*
https://doi.org/10.1186/s43055-024-01284-1

Egyptian Journal of Radiology and Nuclear Medicine

RESEARCH

Open Access

Correlation between chest DW-MRI and 18F-FDG PET/CT in newly diagnosed non-small cell lung cancer (NSCLC)

Abeer Gamal Lotfy[1*], Nora Nabil Abdou[1], Ahmed Mohamed Monib[1] and Rasha S. Hussein[1]

Abstract

Background PET/CT is currently the gold standard for lung cancer staging, and it is also used to identify distant and nodal metastases. High-resolution MRI can also be used to diagnose and provide morphological details about lung cancer. Standardized uptake value 'SUV' calculated from PET/CT gives information about tumor behavior where the SUV reflects metabolic tumor activity. Apparent diffusion coefficient 'ADC' calculated from DW-MRI is a quantitative imaging marker aiming to assess tumor cellularity which reflects tumor behavior. The study aimed to correlate ADC assessed by DW-MRI and metabolic activity determined by SUV max in PET/CT in local and nodal staging of newly diagnosed NSCLC.

Results Our study involved twenty-one patients who were pathologically proven to be NSCLC, 19 males (90.5%) and 2 females (9.5%), with a median age of 61 years (ranging from 37 to 84 years). Among all NSCLC primary mass lesions, we observed a statistically significant inverse correlation between SUV max achieved from PET/CT and ADC max, ADC mean, and ADC min calculated from DW-MR ($r=-0.509$ and $p=0.019$, $r=-0.472$ and $p=0.031$ and $r=-0.434$ and $p=0.049$ for correlation between SUV max of PET/CT and ADC max, ADC mean and ADC min of DW-MR, respectively). Additionally, we observed another statistically significant inverse correlation between SUV max achieved from PET/CT and ADC max, ADC mean, and ADC min calculated from DW-MR in NSCLC mediastinal lymph nodes ($r=-0.699$ and $p=0.011$, $r=-0.58$ and $p=0.048$ and $r=-0.629$ and $p=0.028$ for correlation between SUV max of PET/CT and ADC max, ADC mean and ADC min of DW-MR, respectively).

Conclusions ADC values calculated from DW-MRI might act as a new prognostic tool owing to its significant inverse correlation with SUV max achieved from PET/CT in NSCLC primary mass lesions as well as mediastinal lymph nodes.

Keyword Diffusion-weighted MRI, Magnetic resonance imaging, Positron emission, Tomography computed tomography, Non-small cell lung cancer

Background

Lung cancer remains one of the main causes of cancer-related mortality in the world. Over 80% of cases of primary lung cancer are non-small cell lung cancers (NSCLCs) [1].

PET/CT is a noninvasive functional diagnostic modality that is being employed for plenty of oncological purposes. In cancer patients, especially those with lung cancer, it can early identify pathological changes in affected tissues [2].

Hybrid imaging using PET and CT is a practical method for the initial diagnosis and restaging of lung cancer because it integrates functional and morphological data [3].

*Correspondence:
Abeer Gamal Lotfy
abeergamal1806@gmail.com; abeergamal@med.asu.edu.eg
[1] Department of Diagnostic and Interventional Radiology, and Molecular Imaging, Faculty of Medicine, Ain Shams University, Ramsis St., Abbasia, Cairo 11657, Egypt

PET/CT is currently the gold standard for lung cancer staging and identifying distant and nodal metastases [4].

Nevertheless, there are many drawbacks of PET/CT, including the inability to identify certain well-differentiated lung adenocarcinomas, incorrect categorization of benign inflammatory nodules, higher expenses, and radiation exposure to patients [5].

High-resolution MR imaging provides a sensitive way to distinguish between malignant and benign consolidation. It can accurately identify lung cancers and offer details on the morphology of tumors [6].

DW-MRI principles make use of the random mobility of water molecules in tissues through the apparent diffusion coefficient (ADC) value, a quantitative indicator of the movement of water molecules in biological tissues, which is generally substantially much less in malignant tumors than in benign lesions or normal tissue [7].

Compared to inflammatory reactive tissue or scar tissue, malignant lesions have lower ADC values because of the restricted water diffusion caused by the increased cellular density [8].

Thus, both quantitative imaging markers (SUV and ADC) give information about tumor aggressiveness, with the SUV showing tumor metabolic activity and the ADC assessing tumor cellularity [6].

The study aimed to correlate ADC assessed by DW-MRI and metabolic activity determined by SUV max in PET/CT in local and nodal staging of newly diagnosed NSCLC.

Methods

This was a prospective cross-sectional study that was conducted at our hospital. Twenty-eight patients were enrolled in our study, three patients were excluded because their pathology revealed an inflammatory process as well as other four patients were excluded due to MRI contraindications: three with claustrophobia and one with non-MR compatible pacemaker. Twenty-one patients pathologically proven to have NSCLC who had undergone initial staging with PET/CT, were included in this study between August 2021 and December 2023.

Patients who were subjected to any treatment (chemotherapy or radiotherapy) or surgery apart from biopsy taken before the examination and patients with MR contraindications were excluded. Patients with lung masses proven to be small cell carcinoma were excluded as well.

2 weeks following the biopsy, patients were submitted to PET/CT for initial staging. For our research, we also included axial DWI and T2WI on the chest to assess pulmonary lesions and mediastinal nodal lesions.

18F-FDG PET/CT protocol

Blood glucose levels were assessed before starting the exam to confirm that it was below 200 mg/dl. PET/CT was done using (GE Discovery IQ 5 rings) scanner with (optima 540 16slice) enhanced CT. Intravenous injection of 18F fluorodeoxyglucose was done with an approximate dose of 1 mCi/10 kg followed by saline infusion then image acquisition started one hour later. CT scanning started from the top of the head down to the middle of the thigh with 5 mm slice thickness and parameters of 28–30 mAs and 120 kV, immediately followed by corresponding PET imaging.

The CT images were reconstructed for attenuation correction. Conjoint reading of the images was done simultaneously by two radiologists with 7 and 5 years of experience in nuclear medicine using Advantage Window 4.7 software (AW) (GE Healthcare) workstation.

Interpretation of PET/CT images was performed visually as well as quantitatively. SUV max was measured by placing the ROI around the primary mass lesion and mediastinal lymph nodes that had avid FDG uptake and calculated for each patient according to their body weight.

MRI protocol

MRI of the chest was done in the MRI unit the same day just before the PET/CT examination in 1.5T high field MRI machines (Philips Achieva scanner, Healthcare, Netherlands).

The patient lied supine with a dedicated 16-channel Torso coil solution placed on the chest wall. Axial T2WI images were obtained as well as axial DW-MRI. The expected respiratory motion artifact was accommodated by respiratory gating with a respiratory belt held around the patient's abdomen for breath synchronization.

The time-to-repetition/time-to-echo (TR/TE) values used in T2WI images are 508/80 ms with matrix 256 × 189 and time of 0:21. The time-to-repetition/time-to-echo (TR/TE) values used in DWI images are 4510/66 ms with matrix 120 × 98 and scan time of 02:24 with b value of 0,400,800 800 s/mm^2. For T2WI and DWI, FOV 360 × 302, 5 mm slice thickness, 1 mm gap and 90 flip angle. An automatic pixel-by-pixel ADC map was reconstructed for each patient following the acquisition of the DWI data sets using the MRI unit's standard software. The gray value of every given pixel corresponded linearly with the ADC value. ADC values were assessed manually by placing an elliptical ROI utilizing pixel-wise ADC maps excluding areas of calcifications or necrosis.

Statistical analysis

Data analysis was carried out using IBM SPSS statistics (V. 27.0, IBM Corp., USA, 2020).

For nonparametric quantitative measures, data were expressed as numbers and percentages. For categorized data, they were expressed as median and percentiles.

These tests were conducted:

1. Wilcoxon rank sum test comparison of nonparametric data between two independent groups.
2. For nonparametric data, a ranked Spearman correlation test was used to examine possible associations between each pair of variables within each group.

At 0.05, the probability of error was deemed significant, and at 0.01 and 0.001, it is highly significant.

Results

Patients' characteristics

Overall, our study included 21 patients who were pathologically proven to be NSCLC, 19 males (90.5%) and 2 females (9.5%), with a median age of 61 years (ranging from 37 to 84 years) (Table 1). History of smoking was present in 18 cases (85.7%).

Adenocarcinoma was the most common histological subtype among NSCLC, with squamous cell carcinoma following ($n=11$; 52.4% and $n=10$; 47.6%, respectively) (Table 1).

Of our 21 patients, 14 patients had their primary mass lesion on the right side (66.7%) and 7 patients had their primary mass lesion on the left side (33.3%).

Regarding the primary mass lesions' location, 12 lesions were located in the upper lobe (57.1%), 4 lesions were located in the lower lobe (19.0%), 3 lesions were located hilar (14.3%), one lesion was located in the middle lobe (4.8%), while another one lesion was occupying the middle and the lower lobe (4.8%).

Regarding the oncological staging of these 21 patients, 8 patients were categorized as stage 1 or 2 (38.1%) and the other 13 patients were categorized as stage 3 or 4 (61.9%).

PET/ CT parameters

Primary mass lesion

The 21 primary mass lesions included in our study achieved SUV max of ranged from 2.8 to 49.21 with (median = 12), while the SUV min ranged from 1.17 to 20.69 (median = 5.06) (Table 2).

Mediastinal LN

Of our 21 patients, 12 patients had pathological mediastinal lymph nodes, achieving SUV max ranging from 4.2 to 27.2 (median = 10.75), while SUV min achieved ranged from 1.8 to 22.8 (median = 5) (Table 2).

MRI parameters

Primary mass lesion

The 21 primary mass lesions included in our study had ADC mean ranging from 0.84×10^{-3} to 1.7×10^{-3}mm^2/s (median = 0.96×10^{-3}mm^2/s).

ADC max ranged from 0.98×10^{-3} to 1.84×10^{-3}mm^2/s (median = 1.29×10^{-3}mm^2/s).

Table 1 Patients' characteristics

			Total				Total
Gender	F	Count	2	Pathology	AC	Count	11
		%	9.5%			%	52.4%
	M	Count	19		SCC	Count	10
		%	90.5%			%	47.6%
Total		Count	21	Total		Count	21
		%	100.0%			%	100.0%

Table 2 SUV values achieved in primary mass lesions and mediastinal lymph nodes

	n	Median	Min	Max	Percentiles	
					25	75
Mass SUV max	21	12	2.8	49.21	8.945	20.095
Mass SUV min	21	5.06	1.17	20.69	3.755	8.43
LN SUV max	12	10.75	4.2	27.2	6.8675	13.775
LN SUV min	12	5	1.8	22.8	4.02	7.475

Table 3 Calculated ADC values in primary mass lesion and mediastinal lymph nodes

	n	Median	Min	Max	Percentiles	
					25	75
Mass ADC mean	21	0.96	0.84	1.37	0.89	1.065
Mass ADC max	21	1.29	0.98	1.84	1.1975	1.439
Mass ADC min	21	0.72	0.26	1.28	0.64025	0.8125
LN ADC mean	12	1.1705	0.761	1.762	0.99755	1.3975
LN ADC max	12	1.3515	1.011	1.83	1.2155	1.66
LN ADC min	12	0.936	0.568	1.671	0.6775	1.1745

Table 4 Correlation between ADC values and SUV max of primary mass lesion

	Mass SUV max		
	r	*p*	Sig
Mass ADC mean	−0.472	0.031	S
Mass ADC max	−0.509	0.019	S
Mass ADC min	−0.434	0.049	S

ADC min ranged from 0.72×10^{-3} to $1.28\times10^{-3}mm^2/s$ (median = $0.72\times10^{-3}mm^2/s$) (Table 3).

Mediastinal LN

As previously mentioned, 12 out of the 21 patients had pathological mediastinal lymph nodes, with ADC mean ranging from 0.761×10^{-3} to $1.762\times10^{-3}mm^2/s$ (median = $1.1705\times10^{-3}mm^2/s$).

ADC max ranged from 1.011×10^{-3} to $1.83\times10^{-3}mm^2/s$ (median = $1.3515\times10^{-3}mm^2/s$).

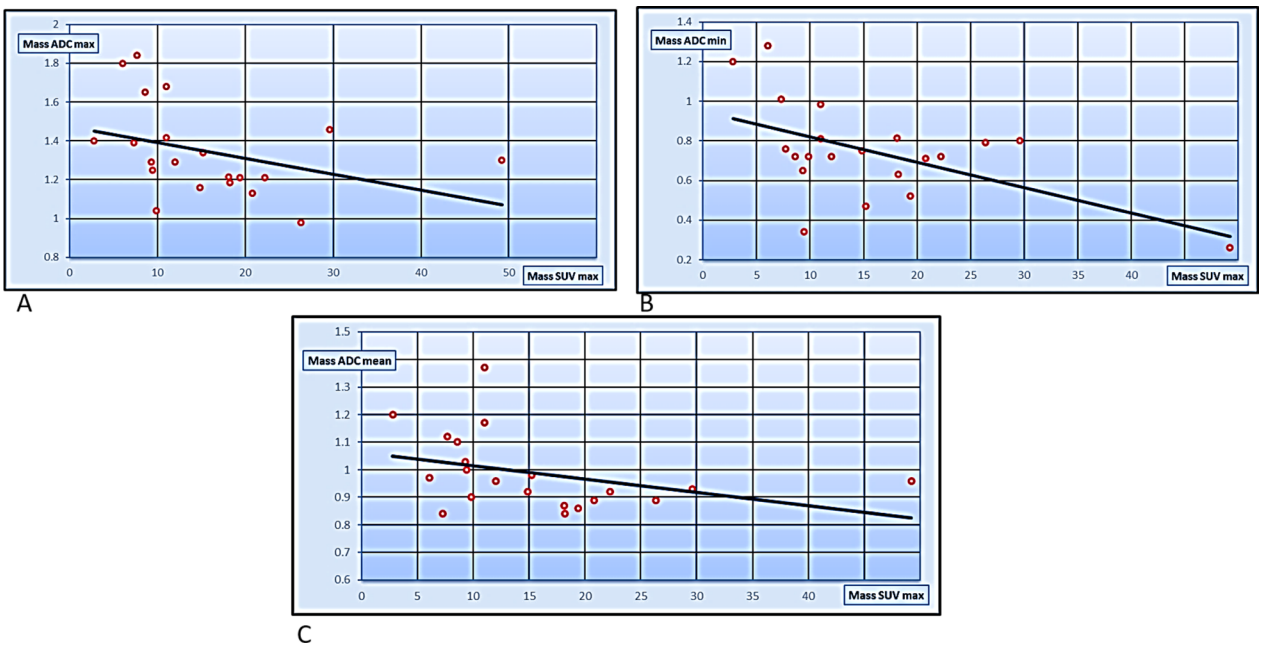

Fig. 1 **A** Regression analysis showing correlation between mass SUV max and mass ADC max in primary mass lesion of all NSCLC cases, **B** regression analysis showing correlation between mass SUV max and mass ADC min in primary mass lesion of all NSCLC cases, **C** regression analysis showing correlation between mass SUV max and mass ADC mean in primary mass lesion of all NSCLC cases

Table 5 Correlation between ADC values and SUV max of mediastinal LNs

	LN SUV max		
	r	*p*	Sig
LN ADC mean	−0.58	0.048	S
LN ADC max	−0.699	0.011	S
LN ADC min	−0.629	0.028	S

ADC min ranged from 0.568×10^{-3} to 1.671×10^{-3}mm^2/s (median = 0.936×10^{-3}mm^2/s) (Table 3).

Correlation between ADC and SUV max of primary mass lesion

Among all NSCLC primary mass lesions, we found an inverse correlation between SUV max achieved through PET/CT and ADC max, ADC mean, and ADC min calculated from DW-MR with Pearson correlation coefficient and *p* value showing statistically significant correlation as shown in Table 4 (Fig. 1).

Correlation between ADC and SUV max of mediastinal LNs

Another significant inverse correlation was detected between SUV max achieved through PET/CT and ADC

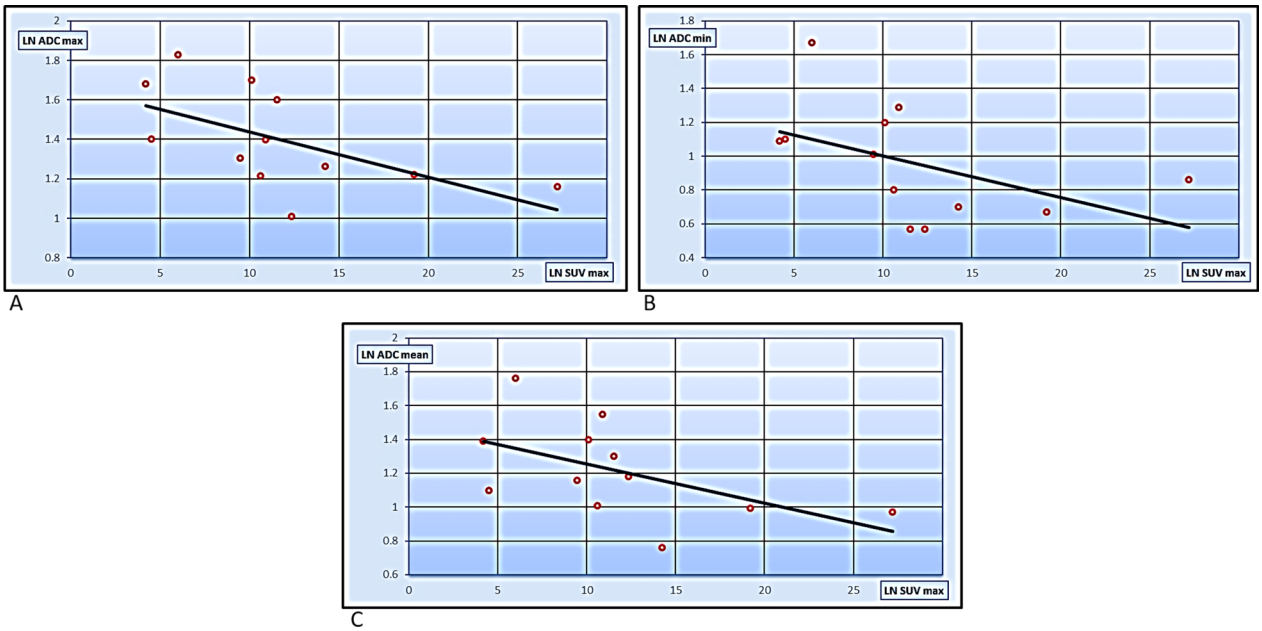

Fig. 2 **A** Regression analysis showing correlation between mass SUV max and mass ADC max in all mediastinal lymph nodes, **B** regression analysis showing correlation between mass SUV max and mass ADC min in all mediastinal lymph nodes, **C** regression analysis showing correlation between mass SUV max and mass ADC mean in all mediastinal lymph nodes

Table 6 Correlation of SUV values of primary mass lesion and mediastinal lymph nodes between AC and SCC

	Patho	*n*	Median	25 Perc	75 Perc	*Z*	*p*	Sig
Mass SUV max	AC	11	11	9.43	19.38			
	SCC	10	15.045	6.9825	24.08	−0.141	0.888	NS
Mass SUV min	AC	11	4.66	3.9	8.13			
	SCC	10	6.315	2.22	10.025	−0.141	0.888	NS
LN SUV max	AC	8	9.79	4.875	11.365			
	SCC	4	16.725	11.5125	25.2	−2.208	0.027	S
LN SUV min	AC	8	4.415	2.4125	5.05			
	SCC	4	12.9	6.425	21.55	−2.717	0.007	HS

max, ADC mean, as well as ADC min of DW-MR in all NSCLC mediastinal LNs with Pearson correlation coefficient and p value showing statistically significant correlation as shown in Table 5 (Fig. 2).

Correlation among Histopathological variants

We found increased median SUV max and SUV min in primary mass lesion of SCC compared to primary mass lesion of AC but of non-significant statistical

Table 7 Correlation of ADC values of primary mass lesion and mediastinal lymph nodes between AC and SCC

	Patho	*n*	Median	25 Perc	75 Perc	*Z*	*p*	Sig
Mass ADC mean	AC	11	0.9	0.87	1.1			
	SCC	10	0.975	0.92225	1.0525	−1.092	0.275	NS
Mass ADC max	AC	11	1.25	1.13	1.418			
	SCC	10	1.365	1.213	1.545	−1.445	0.149	NS
Mass ADC min	AC	11	0.72	0.6305	0.79			
	SCC	10	0.78	0.6575	0.91125	−1.236	0.216	NS
LN ADC mean	AC	8	1.345	1.02005	1.51175			
	SCC	4	1.085	0.9815	1.17575	−1.189	0.234	NS
LN ADC max	AC	8	1.5	1.32775	1.695			
	SCC	4	1.217	1.17275	1.2515	−2.038	0.042	S
LN ADC min	AC	8	0.855	0.594175	1.26675			
	SCC	4	0.976	0.8155	1.096	−0.34	0.734	NS

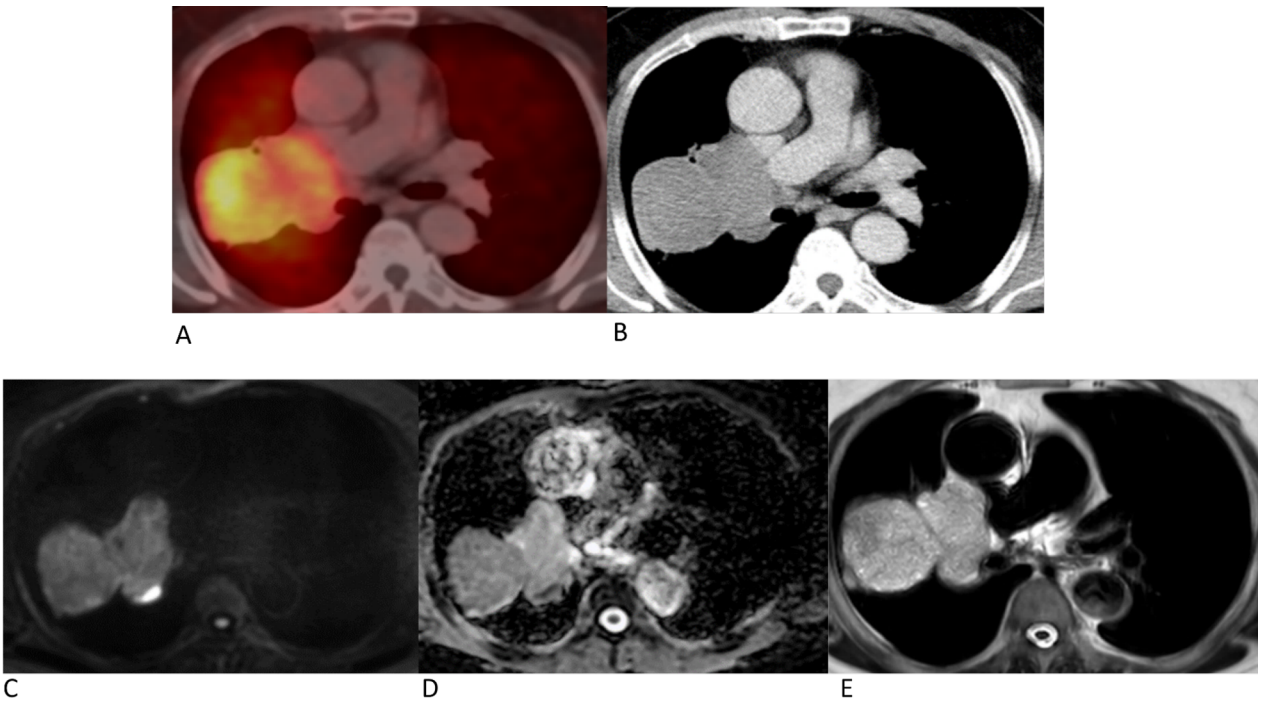

Fig. 3 A 64-year-old male patient with pathologically proven adenocarcinoma with right hilar mass and right hilar lymphadenopathy. **A** Axial PET/CT image shows right hilar mass achieving SUV max of 11 and enlarged right hilar lymph node achieving SUV max of 10, **B** axial CT in soft tissue window showing right hilar mass and enlarged right hilar lymph node, **C** axial DWI of the chest and **D** corresponding ADC map are showing restricted diffusion with ADC min, ADC mean and ADC max values 1.01, 1.37, and 1.68×10^{-3} mm^2/s, respectively, in the right hilar mass and ADC min, ADC mean and ADC max values 1.289, 1.399 and 1.549×10^{-3} mm^2/s, respectively, in the right hilar lymph node, **E** T2WI of the chest showing hyperintense right hilar mass as well as right hilar lymph node

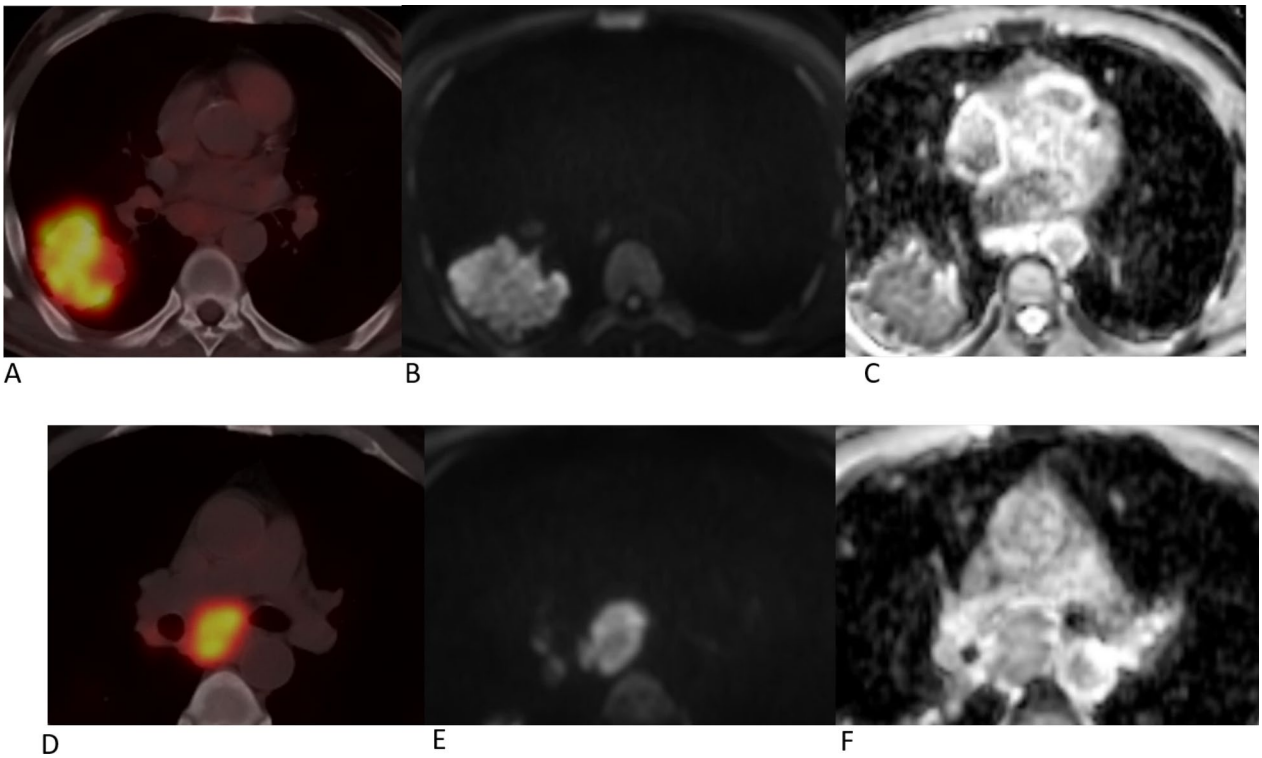

Fig. 4 A 59-year-old male patient with pathologically proven squamous cell carcinoma with right lower lobe mass and mediastinal lymphadenopathy. **A** Axial PET/CT image shows right lower lobe mass achieving SUV max of 22.3, **B** Axial DWI of the chest and **C** corresponding ADC map showing restricted diffusion with ADC min, ADC mean and ADC max of 0.72, 0.92 and 1.21×10^{-3} mm^2/s, respectively, **D** Axial PET/CT image shows subcarinal mediastinal lymphadenopathy achieving SUV max of 19, **E** Axial DWI of the chest and **F** corresponding ADC map showing restricted diffusion in the subcarinal lymph node with ADC min, ADC mean and ADC max of 1.09, 1.16 and 1.22×10^{-3} mm^2/s, respectively

difference. SUV max and SUV min of AC and SCC (median 11 (9.43–19.38) Vs median 15.045 (6.9825–24.08), $p = 0.888$) and (median 4.66 (3.9–8.13) Vs median 6.315 (2.22–10.025), $p = 0.888$), respectively (Table 6).

Significantly increased median LN SUV max among SCC cases in comparison with those AC (median 16.725 (IQ range: 11.5125–25.2) vs 9.79 (4.875–11.365), $p = 0.027$ (Table 6).

Highly significant increased median LN SUV min among SCC cases in comparison with those AC (median 12.9 (IQ range: 6.425–21.55) vs 4.415 (2.4125–5.05), $p = 0.007$ (Table 6).

We found slightly increased median ADC min, ADC max and ADC mean of primary mass lesion of SCC compared to AC but of non-significant statistical difference (Table 7).

Significantly increased median LN ADC max among AC cases in comparison with those SCC (median 1.5 (IQ range: 1.32775–1.695) vs 1.217 (1.17275–1.2515), $p = 0.042$ (Table 7).

Non-significant statistical difference between AC and SCC as regards LN ADC min (median 0.855 (0.594175–1.26675) vs (median 0.976 (0.8155–1.096), $p = 0.734$ (Table 7).

Non-significant statistical difference between AC and SCC as regards LN ADC min (median 1.345 (1.02005–1.51175) vs (median 1.085 (0.9815–1.17575), $p = 0.234$ (Table 7 and Figs. 3, 4, 5, 6).

Discussion

NSCLC is the leading cause of cancer-related mortality each year. It is crucial to early diagnose patients, especially those who may have an unfavorable course of the disease to appropriately modify their treatment plan [9].

The aim of our study was to correlate ADC assessed by DW-MRI and metabolic activity determined by SUV max in PET/CT in local and nodal staging of newly diagnosed NSCLC.

In our study, we had 21 patients with NSCLC and we found a significant inverse correlation between SUV max of PET/CT and ADC of DW-MR in all primary mass

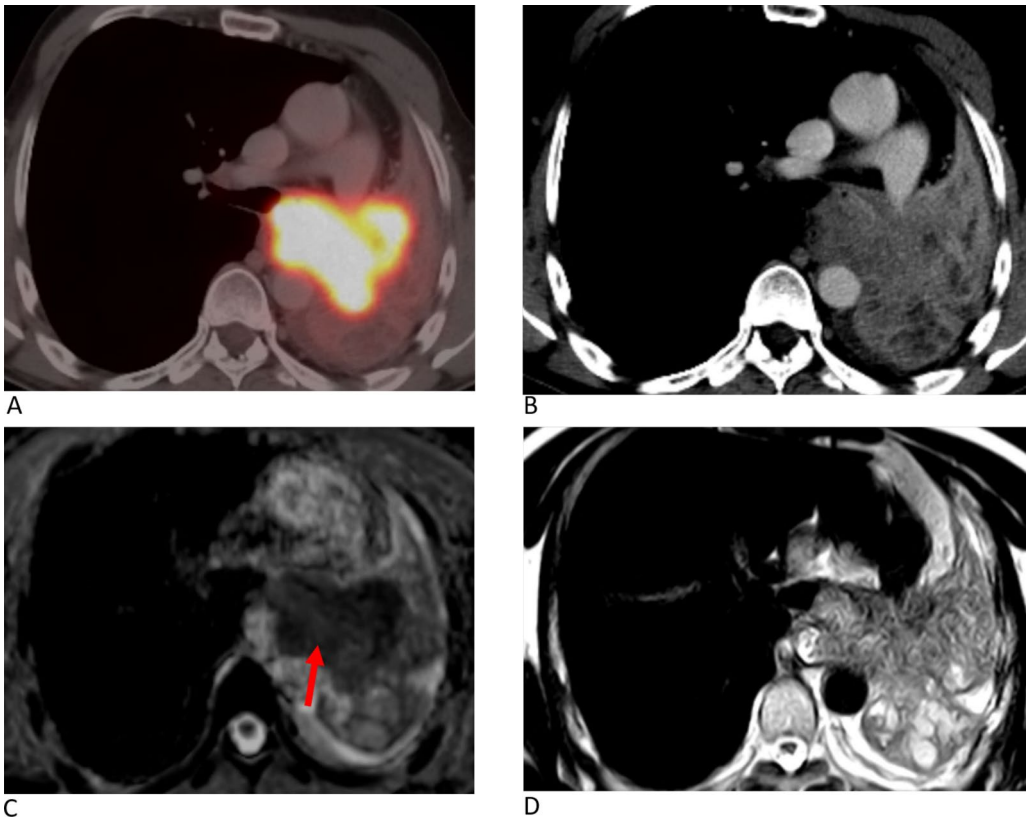

Fig. 5 58-year-old male patient with pathologically proven squamous cell carcinoma showing left central mass with surrounding consolidation/ collapse. **A** Axial PET/CT image shows left central mass achieving SUV max of 49.2 with subsequent non FDG avid left lower lung lobe consolidation/collapse, **B** Axial CT in soft tissue window shows left central mass merging with the subsequent consolidation/ collapse of the left lower lung lobe, **C** Axial ADC map of the chest showing restricted diffusion within the central mass differentiating it from the surrounding subsequent consolidation/ collapse (arrow) with the mass ADC min, ADC mean and ADC max of 0.81, 0.96 and 1.3×10^{-3} mm^2/s, respectively. **D** Axial T2WI of the chest

lesions, regardless of its histological subtypes. This is concordant with studies by Regier et al. [6], Goyal et al. [10], Tyng et al. [11], and Heusch et al. [8] who also found this inverse correlation in 41, 29, 37, and 18 patients, respectively, all of which were NSCLC.

Our study also shows agreement with Tyng et al. [11] whose study showed a negative correlation between SUV max and ADC min for both the primary mass lesion as well as the mediastinal lymph nodes.

We also found an inverse correlation between SUV max and ADC min, ADC mean, and ADC max in all pathological mediastinal LNs regardless of their histological subtypes. This comes in partial agreement with Goyal et al. [10] who observed this inverse correlation in the lymph nodes of adenocarcinoma subtype; however, this inverse correlation was not detected in the lymph nodes of squamous cell carcinoma subtype in their study.

Schaarschmidt et al. [12] also detected a negative correlation between SUV max and ADC mean in mediastinal lymph nodes of 38 NSCLC cases which comes in agreement with our results.

ADC max values in mediastinal lymph nodes of adenocarcinoma cases in our study were higher than that of SCC in mediastinal lymph nodes which comes in agreement with Goyal et al. [10].

Regarding correlation among different histopathological subtypes, the ADC mean values in our study for squamous cell carcinoma were somewhat higher than ADC values for adenocarcinoma in primary mass lesions which comes against Goyal et al. [10] and Matoba et al. [13] who reported lower ADC mean values for squamous cell carcinoma compared to adenocarcinoma.

Usuda et al. [7] investigated the relationship between SUV and ADC with prognostic factors and observed that DW-MRI enabled more precise detection of lymph nodes of NSCLC cases than PET/CT, however, he concluded that ADC was not correlated to prognostic factors and that SUV max might be a better indicator of NSCLC prognosis than ADC.

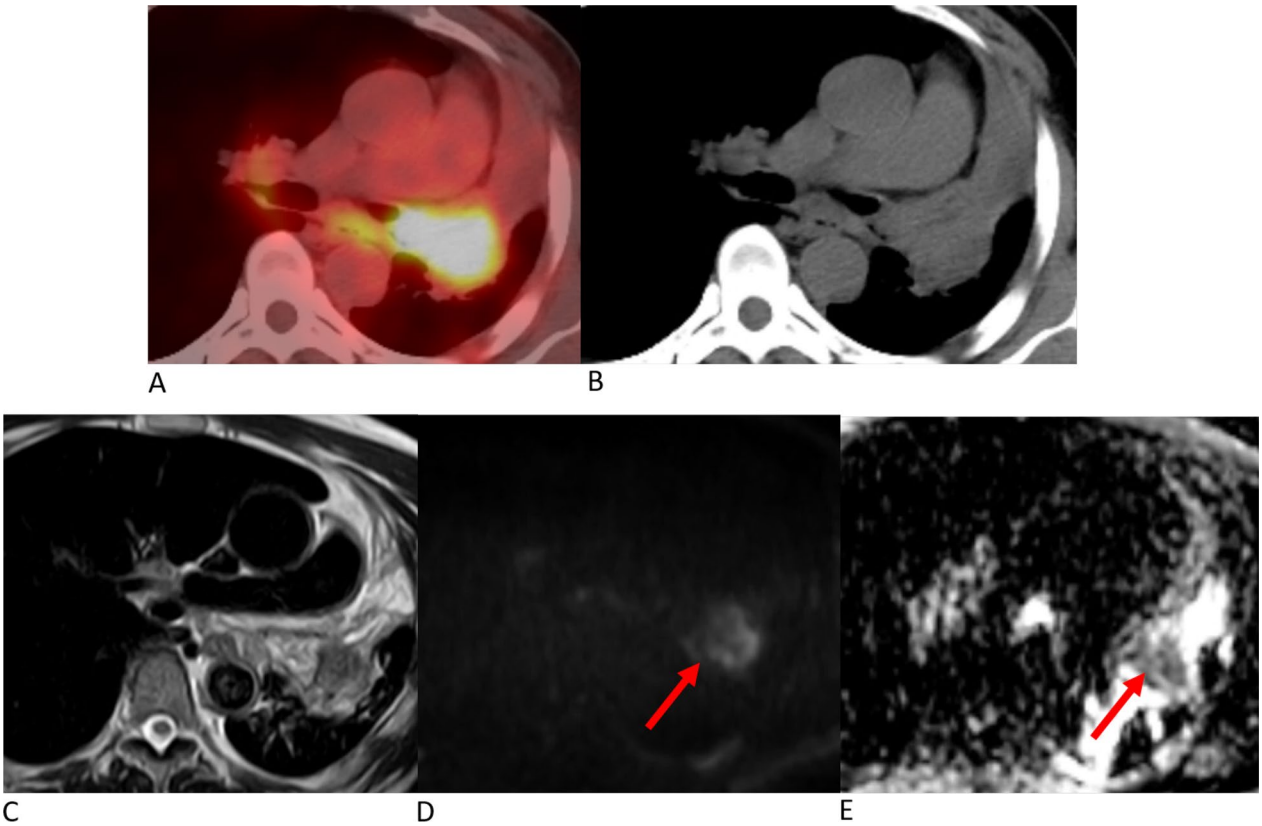

Fig. 6 A 52-year-old male patient with pathologically proven squamous cell carcinoma with left hilar mass, **A** axial PET/CT image shows left hilar mass achieving SUV max of 18.14, **B** axial CT in soft tissue window showing left hilar mass with related lingular consolidation/collapse, **C** axial T2WI of the chest showing hyperintense left hilar mass, **D** axial DWI of the chest and **E** corresponding ADC map are showing restricted diffusion (arrows) with ADC min, ADC mean and ADC max values of 0.815, 1.002 and 1.214×10^{-3} mm^2/s, respectively, in the left hilar mass with facilitated diffusion in the lingular consolidation/collapse

Fifteen NSCLC patients receiving stereotactic body radiation therapy were assessed by Iizuka et al. [14] who found that poor prognosis was linked to high SUV max and a low ADC on pretreatment.

According to Tsuchida et al.'s [15] analysis on 28 patients with NSCLC for treatment response, ADC may be able to help with prognosis in these patients. Also, Ohno et al. [16] found that ADC might be more effective than SUV max in predicting tumor response to therapy in NSCLC cases.

Resistance to treatment manifested with stable SUV max levels is linked to lower overall survival and higher recurrence rates [17].

Yabuuchi et al. [18] demonstrated that ADC values derived from DW-MRI may detect response to treatment early in NSCLC cases receiving chemotherapy. Also, Chang et al. [19] found similar results and demonstrated that ADC values may act as a promising prognostic tool.

Chemotherapy breaks down cell membranes and reduces cell size and density, which makes it easier for molecules to diffuse after treatment starts [20]. Since ADC readings may increase before tumor size decreases, DW-MRI may assess therapy response earlier in advanced NSCLC [21].

All these findings support the relationship between the tumor cellularity measured by DW-MRI through ADC, and glucose metabolism assessed by SUV max, all of which are related to the aggressiveness of tumors.

Although according to our results significant negative correlation between SUV max and different ADC values (min, mean and max) was present, the correlation between SUV max and ADC max of the primary mass lesion as well as the mediastinal lymph nodes were found to be the most statistically significant between the three values, therefore utilizing ADC max value in assessment of tumor cellularity maybe enough to suffice.

There were some limitations to our research. Firstly, the relatively small sample size, and the patients' inclusion criteria were biased on patients' pathology. Also, the study lacks follow-up after therapy to evaluate the potential predictive value of ADC. Additional studies with a larger unbiased sample size are needed as well as

further studies to assess the correlation of ADC and SUV in prognosis and therapeutic response in the population and using other PET/CT parameters.

Conclusions

ADC values calculated from DW-MRI might act as a new prognostic tool owing to its significant inverse correlation with SUV max derived by PET/CT in NSCLC primary mass lesions as well as mediastinal lymph nodes.

Abbreviations

ADC	Apparent diffusion coefficient
DW-MRI	Diffusion-weighted magnetic resonance imaging
FDG	Fluorodeoxyglucose
LNs	Lymph nodes
NSCLC	Non-small cell lung cancer
PET/CT	Positron emission tomography/computed tomography
SUV	Standardized uptake value

Acknowledgements

Not applicable.

Author contributions

All authors contributed to the study conception and design. Material preparation, data collection, and analysis were performed by AGL, NNA, AMM and RSH. The first draft of the manuscript was written by AGL. The authors read and approved the final manuscript.

Funding

No funding was obtained for this study.

Availability of data and materials

The data sets used and/or analyzed during the current study are available from the corresponding author on reasonable request.

Declarations

Ethics approval and consent to participate

The study was approved by the ethical committee of Faculty of Medicine, Ain-Shams University (FMASU REC), under Federal wide assurance No. FWA00017585 (FMASU MD 133/2021).

Consent for publication

Identifying information about participants (patients' identity) did not appear in any part of the manuscript; therefore, consent for publication was not required.

Competing interests

The authors declare that they have no conflict of interest.

Received: 21 March 2024 Accepted: 27 May 2024
Published online: 03 June 2024

References

1. Schiebler ML (2019) Can solitary pulmonary nodules be accurately characterized with diffusion-weighted MRI? Radiology 290(2):535–536. https://doi.org/10.1148/radiol.2018182442
2. Lococo F, Muoio B, Chiappetta M, Nachira D, PetraccaCiavarella L, Margaritora S, Treglia G (2020) Diagnostic performance of PET or PET/CT with different radiotracers in patients with suspicious lung cancer or pleural tumours according to published meta-analyses. Contrast Media Mol Imaging 2020:1–7. https://doi.org/10.1155/2020/5282698
3. Machado Medeiros T, Altmayer S, Watte G, Zanon M, Basso Dias A, HenzConcatto N, HoefelPaes J, Mattiello R, de Souza SF, Mohammed T-L, Verma N, Hochhegger B (2020) 18F-FDG PET/CT and whole-body MRI diagnostic performance in M staging for non–small cell lung cancer: a systematic review and meta-analysis. Eur Radiol 30(7):3641–3649. https://doi.org/10.1007/s00330-020-06703-1
4. Volpi S, Ali JM, Tasker A, Peryt A, Aresu G, Coonar AS (2018) The role of positron emission tomography in the diagnosis, staging and response assessment of non-small cell lung cancer. Ann Transl Med 6(5):95–95. https://doi.org/10.21037/atm.2018.01.25
5. Basso Dias A, Zanon M, Altmayer S, SartoriPacini G, HenzConcatto N, Watte G, Garcez A, Mohammed T-L, Verma N, Medeiros T, Marchiori E, Irion K, Hochhegger B (2019) Fluorine 18–FDG PET/CT and diffusion-weighted MRI for malignant versus benign pulmonary lesions: a meta-analysis. Radiology 290(2):525–534. https://doi.org/10.1148/radiol.2018181159
6. Regier M, Derlin T, Schwarz D, Laqmani A, Henes FO, Groth M, Buhk J-H, Kooijman H, Adam G (2012) Diffusion weighted MRI and 18F-FDG PET/CT in non-small cell lung cancer (NSCLC): Does the apparent diffusion coefficient (ADC) correlate with tracer uptake (SUV)? Eur J Radiol 81(10):2913–2918. https://doi.org/10.1016/j.ejrad.2011.11.050
7. Usuda K, Funasaki A, Sekimura A, Motono N, Matoba M, Doai M, Yamada S, Ueda Y, Uramoto H (2018) FDG-PET/CT and diffusion-weighted imaging for resected lung cancer: correlation of maximum standardized uptake value and apparent diffusion coefficient value with prognostic factors. Med Oncol. https://doi.org/10.1007/s12032-018-1128-1
8. Heusch P, Buchbender C, Köhler J, Nensa F, Beiderwellen K, Kühl H, Lanzman R, Wittsack H, Gomez B, Gauler T, Schuler M, Forsting M, Bockisch A, Antoch G, Heusner T (2013) Correlation of the apparent diffusion coefficient (ADC) with the standardized uptake value (SUV) in hybrid 18F-FDG PET/MRI in non-small cell lung cancer (NSCLC) lesions: initial results. RöFo Fortschritte auf dem Gebiet der Röntgenstrahlen und der bildgebenden Verfahren 185(11):1056–1062. https://doi.org/10.1055/s-0033-1350110
9. Bruckmann NM, Kirchner J, Grueneisen J, Li Y, McCutcheon A, Aigner C, Rischpler C, Sawicki LM, Herrmann K, Umutlu L, Schaarschmidt BM (2021) Correlation of the apparent diffusion coefficient (ADC) and standardized uptake values (SUV) with overall survival in patients with primary non-small cell lung cancer (NSCLC) using 18F-FDG PET/MRI. Eur J Radiol 134:109422. https://doi.org/10.1016/j.ejrad.2020.109422
10. Goyal J, Jajodia A, Koyyala VPB, Bansal A, Batra U, Pasricha S, Puri S, Chaturvedi AK (2023) Correlation of quantitative diffusion-weighted MR parameters and SUVmax from 18-FDG PET-CT in lung cancer: a prospective observational study. Indian J Med Paediatr Oncol 44(04):414–421. https://doi.org/10.1055/s-0042-1754392
11. Tyng CJ, Guimarães MD, Bitencourt AGV, dos Santos LCM, Barbosa PNVP, Zurstrassen CE, Pereira EN, Gross JL, Chojniak R (2018) Correlation of the ADC values assessed by diffusion-weighted MRI and 18F–FDG PET/CT SUV in patients with lung cancer. Appl Cancer Res. https://doi.org/10.1186/s41241-018-0060-1
12. Schaarschmidt BM, Buchbender C, Nensa F, Grueneien J, Gomez B, Köhler J, Reis H, Ruhlmann V, Umutlu L, Heusch P (2015) Correlation of the apparent diffusion coefficient (ADC) with the standardized uptake value (SUV) in lymph node metastases of non-small cell lung cancer (NSCLC) patients using hybrid 18F-FDG PET/MRI. PLoS ONE 10(1):e0116277. https://doi.org/10.1371/journal.pone.0116277
13. Matoba M, Tonami H, Kondou T, Yokota H, Higashi K, Toga H, Sakuma T (2007) Lung carcinoma: diffusion-weighted MR imaging—preliminary evaluation with apparent diffusion coefficient. Radiology 243(2):570–577. https://doi.org/10.1148/radiol.2432060131
14. Iizuka Y, Matsuo Y, Umeoka S, Nakamoto Y, Ueki N, Mizowaki T, Togashi K, Hiraoka M (2014) Prediction of clinical outcome after stereotactic body radiotherapy for non-small cell lung cancer using diffusion-weighted MRI and 18F-FDG PET. Eur J Radiol 83(11):2087–2092. https://doi.org/10.1016/j.ejrad.2014.07.018
15. Tsuchida T, Morikawa M, Demura Y, Umeda Y, Okazawa H, Kimura H (2012) Imaging the early response to chemotherapy in advanced lung cancer with diffusion-weighted magnetic resonance imaging compared to fluorine-18 fluorodeoxyglucose positron emission tomography and computed tomography. J Magn Reson Imaging 38(1):80–88. https://doi.org/10.1002/jmri.23959
16. Ohno Y, Koyama H, Yoshikawa T, Matsumoto K, Aoyama N, Onishi Y, Sugimura K (2012) Diffusion-weighted MRI versus 18F-FDG PET/CT:

performance as predictors of tumor treatment response and patient survival in patients with non-small cell lung cancer receiving chemoradiotherapy. Am J Roentgenol 198(1):75–82. https://doi.org/10.2214/ajr.11.6525
17. Nahmias C, Hanna WT, Wahl LM, Long MJ, Hubner KF, Townsend DW (2007) Time course of early response to chemotherapy in non-small cell lung cancer patients with 18F-FDG PET/CT. J Nucl Med 48(5):744–751. https://doi.org/10.2967/jnumed.106.038513
18. Yabuuchi H, Hatakenaka M, Takayama K, Matsuo Y, Sunami S, Kamitani T, Jinnouchi M, Sakai S, Nakanishi Y, Honda H (2011) Non-small cell lung cancer: detection of early response to chemotherapy by using contrast-enhanced dynamic and diffusion-weighted MR imaging. Radiology 261(2):598–604. https://doi.org/10.1148/radiol.11101503
19. Chang Q, Wu N, Ouyang H, Huang Y (2012) Diffusion-weighted magnetic resonance imaging of lung cancer at 3.0 T: a preliminary study on monitoring diffusion changes during chemoradiation therapy. Clin Imaging 36(2):98–103. https://doi.org/10.1016/j.clinimag.2011.07.002
20. Dudeck O, Zeile M, Pink D, Pech M, Tunn P, Reichardt P, Ludwig W, Hamm B (2008) Diffusion-weighted magnetic resonance imaging allows monitoring of anticancer treatment effects in patients with soft-tissue sarcomas. J Magn Reson Imaging 27(5):1109–1113. https://doi.org/10.1002/jmri.21358
21. Yu J, Li W, Zhang Z, Yu T, Dong L (2014) Prediction of early response to chemotherapy in lung cancer by using diffusion-weighted MR imaging. Sci World J. https://doi.org/10.1155/2014/135841

Publisher's Note